

## Resolution of Sub-Rouse Modes of Polystyrene by Dissolution

K. L. Ngai\*

Naval Research Laboratory, Washington, D.C. 20375-5320

D. J. Plazek

Department of Materials Science &amp; Engineering, University of Pittsburgh, Pittsburgh, Pennsylvania 15261

Received June 24, 2002; Revised Manuscript Received August 28, 2002

**ABSTRACT:** The properties of the softening “glass to rubber” dispersion of two archetypal amorphous polymers, polystyrene and polyisobutylene, appear to differ greatly. Previously, these differences have been explained by the larger intermolecular coupling between the repeat units in executing the local segmental motions in polystyrene than polyisobutylene. Dissolution of polystyrene into a solvent with a lower glass temperature certainly diminishes the intermolecular coupling and could make the softening dispersion of the polystyrene solution resemble bulk polyisobutylene. Creep compliance measurements of solutions of polystyrene in tri-*m*-tolyl phosphate are used to show that this expectation is the case. At 17% polystyrene, the properties of the softening dispersion of the solution are nearly identical to that of bulk polyisobutylene, including the appearance of a resolved sub-Rouse mode.

## I. Introduction

Measurements of the viscoelastic behavior of bulk polymers showed that polystyrene (PS) and polyisobutylene (PIB) differ greatly in the “glass to rubber” softening dispersion.<sup>1–11</sup> PS has much narrower softening dispersion than PIB and deviates greatly from that predicted by the Rouse model extended to undiluted polymers.<sup>2</sup> On the other hand, the softening dispersion of PIB is much broader and shows smaller deviations from the Rouse model. Other differences between viscoelastic properties of PS and PIB have been summarized in refs 9 and 10. Shear creep compliance,  $J(t)$ , data of PS and PIB samples with nearly the same degree of polymerization show that the softening dispersion of PIB is wider by a few more decades than that of PS.<sup>12</sup> In another way, this difference is shown in Figure 1 where we compare the retardation spectra,  $L(\lambda/a_T)$ , of high molecular weight PS and PIB, where  $\lambda$  is the retardation time and  $a_T$  is the temperature shift factor.  $L$  is defined in

$$J(t) = J_g + \int_{-\infty}^{\infty} L(\lambda)(1 - e^{-t/\lambda}) d \ln \lambda + \frac{t}{\eta} \quad (1)$$

and is obtained from the  $J_r(t)$  data by a numerical procedure.<sup>13</sup> The shift factors  $a_T$  for the two polymers are chosen such that position of the first peak of  $L$ , corresponding to the Rouse modes and indicating the end of the softening dispersion, of PS and PIB occurs at the same reduced retardation time. It is clear by inspection of Figure 1 that  $L$  of PS (open triangles) has a much steeper rise to the peak, and hence the width of the softening dispersion of PS is considerably smaller than that of PIB (open circles). There are several other differences in the softening dispersion between PIB and PS.<sup>9–12</sup> An example is the loss tangent,  $\tan \delta \equiv J''(\omega)/J'(\omega)$ , which exhibits two peaks in the softening dispersion of high molecular weight PIB,<sup>5,6,9,10</sup> while there is

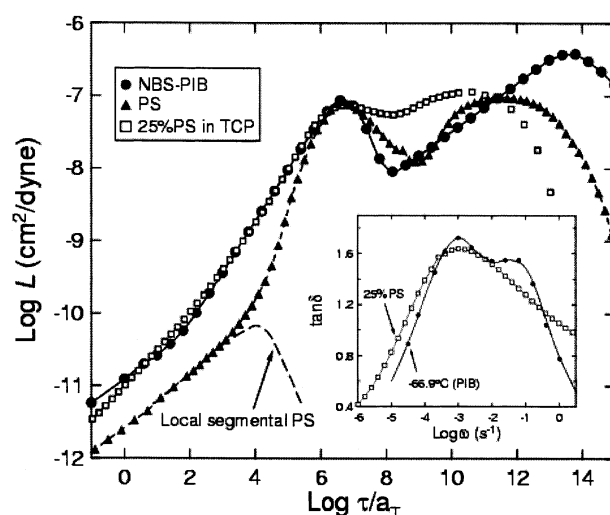


**Figure 1.** Comparison of the retardation spectra  $L$  of a high molecular weight PS (filled triangles), a 25% PS solution in TCP (open squares), and PIB (filled circles). The shift factors are arranged such that the maximum of the first peak occurs at the same reduced frequency for all three samples. Downward vertical shifts of 0.869 and 1.39 of  $\log L$  have been applied respectively to PS and 25% PS solution to make all data have about the same height at the first maximum. The disparity in width of the softening dispersion of bulk PS and PIB is clear. The small peak near the bottom (dashed line) is the contribution to  $L$  from the local segmental motion in bulk PS. The inset shows isothermal data of  $\tan \delta$  of PIB in the softening region at  $-66.9^\circ\text{C}$  and  $\tan \delta$  of the 25% PS solution in TCP obtained from a reduced recoverable compliance curve after applying time-temperature superposition to the limited isothermal data.<sup>13,26</sup>

only one peak for high molecular weight PS and other polymers that had been studied.<sup>10,14,15</sup> The lower frequency  $\tan \delta$  peak in PIB corresponds to the Rouse modes. The extra peak at higher frequencies found in PIB but not in PS comes from motion of chain segments with length scales intermediate between the Gaussian submolecule of Rouse and the local segmental motions LSM.<sup>9,10,16</sup> Williams<sup>17</sup> showed that the Gaussian submolecular model of Rouse can account only for the

\* Corresponding author: telephone 202 7676150; Fax 202 7670546; e-mail Ngai@estd.nrl.navy.mil.

viscoelastic behavior in the longer relaxation time portion of the glass–rubber softening dispersion. He estimated that for high molecular weight PS the compliances contributed by the Rouse modes are higher than about  $10^{-7} \text{ Pa}^{-1}$ . On the other hand, recent studies have determined that the compliances contributed by the local segmental motion in amorphous polymers, which is responsible for the glass temperature, are typically<sup>10,18–20</sup> not higher than about  $5 \times 10^{-9} \text{ Pa}^{-1}$ . Thus, the extended Rouse model has to be augmented by new molecular mechanisms that contribute to compliances in the gap,  $5 \times 10^{-9} < J_r < 10^{-7} \text{ Pa}^{-1}$ . The molecular motions in the new mechanisms involve chain lengths smaller than the submolecule but larger than the local segmental motions, and naturally we called them the “sub-Rouse modes”.<sup>9,10</sup> Actually, the first direct evidence of sub-Rouse modes in PIB was found by dynamic light scattering.<sup>21,22</sup> From the fact that local segmental motion is enthalpic and the Rouse modes are entropic, we may expect the intermediate sub-Rouse modes to have part of each character. The softening dispersion of PIB thus has three contributions: (i) the local segmental motions (LSM) responsible for  $J(t)$  from  $J_g \approx 10^{-9} \text{ Pa}^{-1}$  up to about  $J_{sa} \approx 5 \times 10^{-9} \text{ Pa}^{-1}$ , (ii) the sub-Rouse modes from  $J_{sa}$  up to somewhere near  $J_{sr} \approx 10^{-7} \text{ Pa}^{-1}$ , and (iii) the Rouse modes from  $J_{sr} \approx 10^{-7} \text{ Pa}^{-1}$  up to the plateau level.<sup>10,18–20</sup> The lack of a higher frequency peak in  $\tan \delta$  of PS in the softening dispersion to reflect the existence of the sub-Rouse modes is rationalized by the inability to resolve it due to the significantly narrower softening dispersion of PS relative to that of PIB.

The origin of the various differences in the viscoelastic properties between PS and PIB has been traced to a more fundamental observed anomalous property of amorphous polymers; i.e., the shift factor of the LSM is more sensitive to temperature changes than that of the Rouse modes. There is direct experimental evidence for this difference from the breakdown of thermorheological simplicity of the softening dispersion.<sup>10,12,18–25</sup> Furthermore, the difference in the temperature dependences of the LSM and the Rouse modes is larger in PS than in PIB,<sup>12</sup> and because of this, the narrower width of the softening dispersion of PS follows from greater encroachment of the time scale of the LSM toward the Rouse modes, resulting in greater overlap. Theoretically, an explanation of this thermorheological complexity of the softening dispersion has been offered by the coupling model.<sup>12,18–25</sup> As given in more detail in the next section, the explanation is based on stronger intermolecular coupling between the repeat units of PS than of PIB in executing the LSM because PS has a bulky phenyl ring attached to a carbon in the main chain while PIB has a more compact symmetric backbone. If indeed this were the cause, then we can make the softening dispersion of PS resemble that of PIB by some means that reduces the intermolecular coupling of LSM in PS. One such means is diluting PS by a solvent that has a lower glass temperature. Addition of the solvent increases the average separation between the repeat units and therefore reduces their intermolecular coupling. The purpose of this work is to show that indeed various properties of the softening dispersions of solutions of PS in *m*-tricresyl phosphate (*m*-TCP = tri-*m*-tolyl phosphate) approach that of PIB with continued addition of the solvent, and at some solvent concentration the softening dispersion of the PS solution in many respect resembles

that of PIB. New measurements were made to augment previous measurements<sup>13,26</sup> for the purpose of this study.

## II. Reason for the Difference between PS and PIB

The local segmental motions that are responsible for the glass temperature of the amorphous polymer are located at the short time (high frequency) part of the glass–rubber softening dispersion. They are observed in enthalpy relaxation measurements and dilatometry by the time-dependent contractions observed in physical aging experiments in the neighborhood of  $T_g$ . The local segmental motions (LSM) in amorphous polymers, which determine the molecular packing and thus the glass temperature,  $T_g$ , impart mobility to motions with longer length scales and therefore is a basic mechanism of the viscoelasticity of polymers. In previous studies we were able to isolate the contribution of the LSM to the softening dispersion. Experimental data<sup>10,12,18–25</sup> have shown that the LSM ( $\alpha$ -relaxation) contributes a compliance that is well approximated by the second term in

$$J_\alpha(t) = J_g + (J_{e\alpha} - J_g)[1 - \exp(-(t/\tau_\alpha)^{1-n_\alpha})] \quad (2)$$

where  $0 < (1 - n_\alpha) \leq 1$  and the steady-state recoverable compliance,  $J_{e\alpha}$ , has been determined only for low molecular weight polymers and is approximately  $J_{e\alpha} \approx 4.0J_g$  for polystyrene<sup>20</sup> and  $J_{e\alpha} \approx 5.0J_g$  for poly(methylphenylsiloxane).<sup>18</sup>  $J_g = 9 \times 10^{-10} \text{ Pa}^{-1}$  for PS and  $5.4 \times 10^{-10} \text{ Pa}^{-1}$  for PMPS. These values of  $J_{e\alpha}$  were deduced by taking advantage of an effect caused by the encroachment of the time scale of the LSM toward the Rouse modes as temperature is decreased.<sup>10,12,18,23</sup> The effect in low molecular weight polymers entirely eliminates the polymeric modes contribution to the recoverable compliance to leave only the local segmental contributions (see Figures 50–52 of ref 10) as temperature is decreased to approach  $T_g$ . Donth and co-workers<sup>27,28</sup> have made extensive shear dynamic modulus measurements and confirmed the presence of a shoulder in their retardation spectra,  $L(\tau/a_T)$ , in several polymers including PVAc and polystyrene. The shoulder is sufficiently prominent in the retardation spectrum of polystyrene to permit the contribution of the local segmental motion,  $L_\alpha$ , to be isolated for the first time<sup>20</sup> in any high molecular weight amorphous polymer and is shown by the small peak in Figure 1. This result for  $L_\alpha$  is consistent with the retardation spectra of the LSM deduced from low molecular weight polystyrene using the “encroachment effect” near  $T_g$ .

Several experimental studies have shown that near  $T_g$  the shift factor,  $a_{T,\alpha}$ , of the LSM ( $\alpha$ ) changes much more rapidly with temperature than the shift factor,  $a_{T,R}$ , of the Rouse modes.<sup>10,12–14,18–25</sup> Consequently, with a decrease in temperature, the contribution of the LSM modes to the retardation spectrum (seen at shorter times by the small peak of PS in Figure 1) shifts by the larger amount to longer times than the retardation time spectrum of the *R*-modes (located at longer times in the vicinity of the first peak of PS in Figure 1). The “encroachment” of the LSM toward the *R*-modes decreases the width of the softening dispersion determined from the master curve obtained by time–temperature superposition of isothermal data or from  $L(\tau/a_T)$  in Figure 1. Experimental data have shown that the

encroachment is more severe in PS than in PIB,<sup>10,12</sup> and this experimental fact immediately explains the narrower width of the softening dispersion found in PS than in PIB.

A theoretical explanation of the encroachment effect has been provided by the coupling model<sup>29,30</sup> prediction:<sup>12,18–20</sup>

$$a_{T,\alpha} = (a_{T,0})^{1/(1-n_\alpha)} \quad (3)$$

where  $n_\alpha$ , the LSM coupling parameter, is the same as that in eq 2 and is a measure of the intermolecular coupling between the repeat units in executing the LSM. The Rouse modes in the softening dispersion are independent of each other (i.e., no effect due to entanglement), and they are entropic in nature; hence, there is no coupling<sup>20</sup> and

$$a_{T,R} = a_{T,0} \quad (4)$$

Here  $a_{T,0}$  is the primitive (before coupling is considered) shift factor in the coupling model and is the same for the LSM and the Rouse modes. Light scattering measurements<sup>31</sup> as well as creep compliance data<sup>20</sup> have determined  $n_\alpha$  for high molecular weight PS to have the relatively large value of 0.64. On the other hand, light scattering measurement on high molecular weight PIB<sup>21,22</sup> has found a smaller value of  $n_\alpha$  equal to 0.45. On comparing eqs 3 and 4, we can conclude that for both polymers the retardation/relaxation times of the LSM  $\alpha$ -mode shifts with decreasing temperature to longer times much more than the Rouse modes (i.e., encroachment). Moreover, it follows from eq 3 that, because of larger  $n_\alpha$ , the encroachment effect at temperatures near  $T_g$  is larger in PS than in PIB, and the separation between the LSM and the Rouse modes at  $T_g$  is correspondingly smaller. Thus, the narrower softening dispersion of PS compared with PIB is explained.

Coupling between the PS repeat units, and hence  $n_\alpha$ , is expected to decrease monotonically with the addition of a diluent with a lower  $T_g$ , due to the increasing separation between the slower repeat units. The coupling model explanation of the different widths of the softening dispersion of PS and PIB hinges on the fact that PS has a larger  $n_\alpha$  than PIB. With decrease of  $n_\alpha$  of PS on dissolution, we expect that the width of the softening dispersion of the PS solutions will increase with addition of a diluent. At some optimum polymer concentration, the softening dispersion of the PS solution may resemble bulk PIB, not only in width but also in other properties such as the emergence of the sub-Rouse modes found in bulk PIB<sup>9,10,21,22</sup> but not in bulk PS.<sup>10,14</sup>

### III. Experimental Data

Shear creep compliance,  $J(t)$ , and the recoverable compliance,  $J_r(t) = J(t) - t/\eta_0$ , data were obtained previously<sup>13,26</sup> on solutions in tri-*m*-tolyl phosphate (TCP) of PS with  $M_w = 860\,000$  and  $M_w/M_n = 1.1$  (designated PC-6a) over a broad concentration range from the undiluted polymer down to 1.25 wt % PS. The data and the magnetic-bearing creep apparatus used for the measurement were described in a previous publication.<sup>26</sup> From the data collected, the trend of broadening of the softening dispersion with decreasing concentration of PS can be observed. At the time when these measurements were performed, emphasis was not placed

in resolving the various viscoelastic mechanisms in the softening dispersion like we did recently with PIB.<sup>9</sup> Isothermal  $J_r(t)$  data of the 25% PS solution were taken from about half a second to slightly above  $10^4$  s, a limited portion of the accessible time range. Data taken at the various temperatures were superposed by translations along the  $\log t$  axis. A reduced plot obtained from the  $J_r(t)$  data as a function of the reduced time,  $t/a_T$ , was used to calculate the retardation spectrum  $L(\tau/a_T)$  of the 25% PS solution, which is shown in Figure 1. The reduced time here is chosen such that the maximum of the first peak occurs at the same place as that of bulk PS. It is clear that the softening dispersion of the 25% PS solution is significantly broader than bulk PS and approaches that of PIB. However,  $\tan \delta$  calculated from the data of the 25% PS solution as a function of  $t/a_T$  exhibits only one broad peak (open squares in the inset of Figure 1), in contradistinction with the two-peak structure found in  $\tan \delta$  of PIB from isothermal data<sup>9</sup> taken at  $-66.9^\circ\text{C}$  (filled circles in the inset of Figure 1). There are two possible causes for the nonappearance of the higher frequency peak in  $\tan \delta$  of the 25% PS solution. The first is that the softening dispersion of the 25% PS solution is still not broad enough to resolve the two peaks. The second is the fact that  $\tan \delta$  of the 25% PS solution is obtained from reduced  $J_r(t)$  data of an earlier work<sup>13,26</sup> and not from isothermal data. Previously, we have shown<sup>9</sup> in the case of PIB that, although isothermal data give rise to two peaks to  $\tan \delta$ , the higher frequency peak or shoulder can no longer be resolved in the  $\tan \delta$  calculated from the reduced data  $J_r(t/a_T)$ , obtained after time–temperature superposition. Thus, the previous measurements on the 25% PS solution cannot be used to compare in detail the viscoelastic properties of its softening dispersion with that of PIB.

A thorough comparison requires new isothermal measurements that take advantage of the full range of nearly 6 decades in time of the creep apparatus. We chose to make such measurement on a freshly prepared 17% PS solution because its softening dispersion would be even broader than that of the 25% PS solution, making the resolution of the higher frequency peak easier. The same polymer PC-6a was used to make the 17% PS solution. Figure 2 shows the isothermal  $J_r(t)$  data in the softening region at four temperatures ( $-57.7$ ,  $-54.0$ ,  $-49.25$ , and  $-36.1^\circ\text{C}$ , filled squares) over a time scale extending over 6 decades up to about  $10^6$  s, an improvement over the previous measurements<sup>13,26</sup> which cover only 4 decades of creep time up to about  $10^4$  s. Like in any miscible blends, polystyrene and TCP have their separate local dynamics, although the local dynamics of each component is modified by the presence of the other.<sup>32,33</sup> Consequently, they can have two different glass temperatures.<sup>26,33</sup> In this work we are interested in the viscoelastic response of polystyrene but not the solvent. For this reason, the measurement temperatures of the 17% PS solution are all above the glass temperature of the polystyrene component, which is  $-60^\circ\text{C}$ . The response of TCP can only be seen at lower temperatures and/or shorter times not explored in this work. For comparison, the data of a high molecular weight PIB at six temperatures ( $-74.0$ ,  $-66.9$ ,  $-52.0$ ,  $-36.0$ ,  $-11.0$ , and  $27.0^\circ\text{C}$ , open circles) are shown also in Figure 2. The compliance of the 17% PS solution is higher than the bulk PIB as expected, but they have similar time dependence in the softening dispersion. The



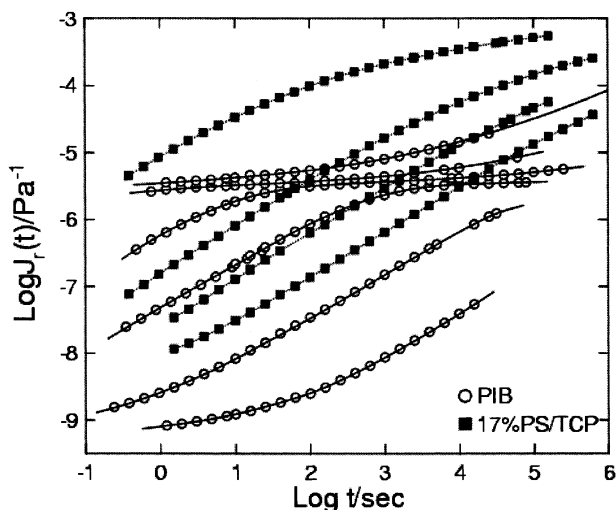


**Figure 2.** Recoverable creep compliance data in the softening region of the 17% PS solution in TCP at  $-57.7$ ,  $-54.0$ ,  $-49.25$ , and  $-36.1$  °C (filled squares). Shown for comparison are the recoverable compliance data of PIB at six temperatures,  $-74.0$ ,  $-66.9$ ,  $-52.0$ ,  $-36.0$ ,  $-11.0$ , and  $27.0$  °C (open circles).

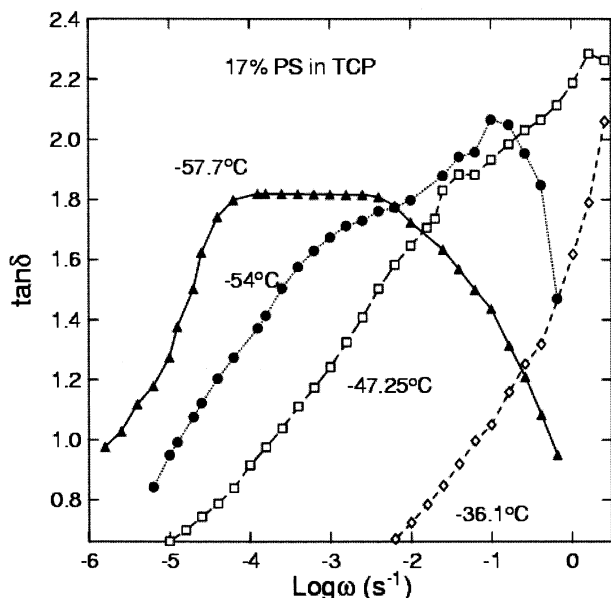


**Figure 3.** Isothermal  $\tan \delta$  of the 17% PS solution in TCP in the softening region at  $-57.7$ ,  $-54.0$ ,  $-49.25$ , and  $-36.1$  °C.

real and imaginary parts of the dynamics compliances,  $J(\omega)$  and  $J''(\omega)$ , are obtained from  $J_r(t)$  from the empirical relations<sup>34,35</sup> given by

$$J(\omega) = [1 - m(2t)]^{0.8} J_r(t)|_{t=1/\omega} \quad (5)$$

$$J(\omega) = [m(2t/3)^{0.8} J_r(t) + 1/\omega\eta_0|_{t=1/\omega}] \quad (6)$$

where  $m = d \log J_r(t) / d \log t$ . From the dynamic compliances,  $\tan \delta$  is calculated as the ratio  $J''(\omega)/J(\omega)$  for four temperatures and shown in Figure 3. The plots of  $\tan \delta$  at  $-47.25$ ,  $-54.0$ , and  $-57.7$  °C show two peaks within the softening dispersion, indicating the existence of two distinct viscoelastic mechanisms therein.

#### IV. Comparing 17% PS Solution with PIB

The most obvious difference of the softening dispersions in bulk PS and PIB is their widths (see Figure 1). We have seen in Figure 2 that the time dependences of

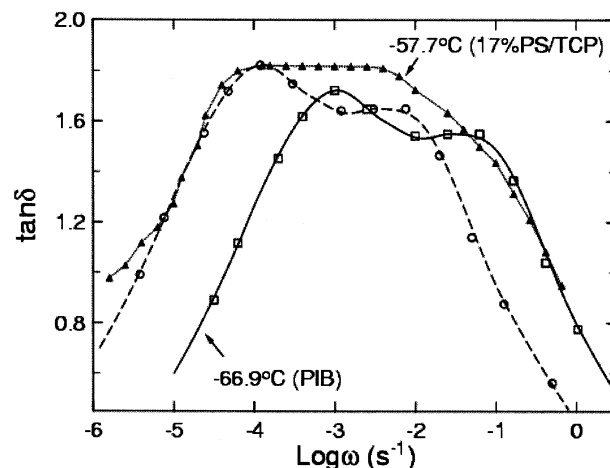


**Figure 4.** Comparison of isothermal  $\tan \delta$  of the 17% PS solution in TCP at  $-57.7$  °C (filled triangles) and isothermal  $\tan \delta$  of PIB at  $-66.9$  °C (open squares) in the softening region. The open circles are  $\tan \delta$  of PIB at  $-66.9$  °C after the first peak is shifted horizontally and scaled vertically to match the position and height of the first peak of the 17% PS solution. The lines connecting the data points of each set are drawn to guide the eyes.

the recoverable compliances in the softening dispersion of the 17% PS solution and bulk PIB are similar. This similarity already indicates that the width of the softening dispersion of bulk PS can be made nearly the same as PIB by addition of the solvent TCP to make solutions with PS concentration in the range 17–25 wt %.

A more subtle difference between the softening dispersions of bulk PS and PIB is the appearance of a single peak in  $\tan \delta$  of PS,<sup>10,13</sup> while two peaks are found in  $\tan \delta$  of PIB. The lone peak in  $\tan \delta$  of PS comes from the Rouse modes, although its shape changes with temperature. Such a breakdown of thermorheological simplicity is due to the difference between the shift factors of the LSM and the Rouse modes and the presence of a hidden viscoelastic mechanism at intermediate times with temperature dependence also not the same as the Rouse modes, which cannot be resolved in PS even in  $\tan \delta$  because of the narrow width of its softening dispersion. A natural origin of the hidden mechanism is the existence of polymeric (sub-Rouse) modes<sup>9,10,15,17,18,20</sup> with length scales intermediate between the local segmental modes and the Gaussian submolecule necessary for the definition of the Rouse modes. The much wider softening dispersion of PIB enables the sub-Rouse modes to be resolved as the second peak of  $\tan \delta$  at higher frequencies as shown in the inset of Figure 1 and in Figure 4 by an example from isothermal recoverable compliance data of PIB taken at  $-66.9$  °C (open squares). It is clear from the plots in Figure 4 that the two-peak structure of  $\tan \delta$  of PIB is recaptured in PS by diluting it to form a 17% PS solution. A more quantitative comparison between the data is obtained by shifting the data of PIB in Figure 4 horizontally along the frequency axis and scaling them by a constant factor to place the lower frequency Rouse peak at the same position as that of the 17% PS solution. This comparison shows that the separation between the two peaks is about the same for PIB and 17% PS solution.

A difference between undiluted PS and PIB can be seen in the temperature dependences of the viscosity and the shift factor of  $J_r(t)$  in the softening dispersion.

While these two temperature dependences are quite different in bulk PS,<sup>10</sup> particularly at lower temperatures near  $T_g$ , they are comparable in PIB.<sup>10,36</sup> In this respect, the 17% PS solution behaves like PIB because the temperature dependence of the measured viscosity (not shown) differs little from that of the shift factor of  $J_r(t)$  in the softening dispersion. The parameters  $C$  and  $T_\infty$  in the term  $(C/2.303)/(T - T_\infty)$  in the Vogel–Fulcher–Tammann–Hesse equation that determines the temperature dependence are respectively equal to 3010 C and  $-132$  C for the viscosity and 3030 C and  $-127$  C for the shift factors of  $J_r(t)$  in the softening dispersion. This can be seen to be true for all TCP solutions of PS at polymer concentrations of 40% or less,<sup>26</sup> except for the values previously presented for the 25% PS solution, which are considered to be spurious due to small number of viscosity determinations for this solution (see remarks in Table 1 of ref 26).

An objective way to compare the temperature dependence of the shift factor,  $a_T$ , of viscoelastic data near and above  $T_g$  of different polymers, having different glass temperatures, is to use normalized reciprocal temperature variables like  $T_g/T$  or normalized temperature difference variables like  $(T - T_g)/T_g$ . In the comparison made before,<sup>37</sup> the shift factors were all determined from recoverable creep compliance measurements. Near  $T_g$ , the measured  $J_r(t)$  at times below 100 s comes predominantly from local segmental motions (LSM), and the dependence of the shift factors  $a_T(T)$ , where  $T_g$  is the reference temperature, on  $T_g/T$  near  $T_g/T = 1$  truly reflects that of the retardation time  $\tau$  of the LSM in eq 2. In other words,  $a_T(T)$  can be identified with  $a_{T,\alpha}$ , appearing in eq 3. Therefore, the steepness index, defined<sup>37,38</sup> by  $S$  or  $m \equiv d[\log(a_T(T))/d(T_g/T)]$  and evaluated at  $T = T_g$ , is a true characteristic of the LSM. On the other hand, at higher temperatures the measured  $J_r(t)$  arises increasingly from the sub-Rouse modes and the Rouse modes, and there the dependence of  $a_T(T)$  on  $T_g/T$  is no longer a characteristic of the LSM. These data of PS and PIB are replotted in Figure 5, and they show that near  $T_g/T = 1$  PS has a more sensitive  $T_g$ -scaled temperature dependence than PIB. The value of  $m$  of PS reported here is 152, which is significantly larger than 58 for PIB. In fact, PIB has the smallest  $m$  among many amorphous polymers.<sup>37,38</sup> However, the sensitivity of the dependence of  $a_T(T)$  on  $T_g/T$  as well as the value of  $m$  decreases when TCP is added to PS, and the change increases with the TCP content. These trends can be seen in Figure 5 where  $a_T(T)$  obtained from the recoverable compliance data of 50%, 25%, and 17% PS solutions are plotted against  $T_g/T$ . The values of  $T_g$  of the 50%, 25%, and 17% PS solutions are  $-12$ ,  $-52$ , and  $-60$  °C, respectively. The values of  $m$  for 50%, 25%, and 17% PS solutions are 81, 65, and 61, respectively. Thus, the dependence of  $a_T(T)$  on  $T_g/T$  and the value of  $m$  of the 17% PS solution come close to that of PIB. Incidentally,  $T_g$  of PIB is  $-73$  °C,<sup>39</sup> which is near that of the 17% PS solution.

A correlation between  $m$  and  $n_\alpha$  that appears in the exponent  $(1 - n_\alpha)$  in both eqs 2 and 3 has been established for the class of amorphous polymers including PS and PIB, as well as for other classes of nonpolymeric glass-formers.<sup>38</sup> Applying this correlation to include the 17% PS solution, the fact that it and PIB has nearly the same  $m$  implies that it has nearly the same  $n_\alpha$  as PIB, which has been determined<sup>21,22</sup> to be 0.45. This deduction that PIB and the 17% PS solution has

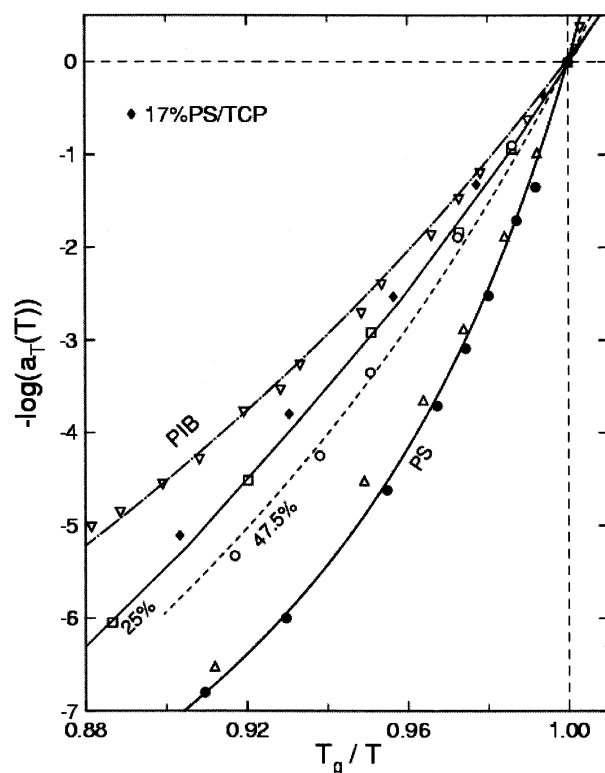


**Figure 5.** Plot of the shift factors  $a_T(T)$  referred to  $T_g$  vs  $T_g/T$  for two high molecular weight PS samples (filled circles for A-25 and open triangles for PC-6A), 50% PS/TCP (open circles), 25% PS/TCP (open squares), 17% PS/TCP (filled diamonds), and PIB (filled triangles). The lines are calculated from the Vogel–Fulcher–Tammann–Hesse fits to the data. Only data are shown for the case of the 17% PS/TCP for the sake of clarity.

approximately the same  $n_\alpha$  together with eqs 3 and 4 indicates that the difference between the shift factors  $a_{T,\alpha}$  and  $a_{T,R}$  is nearly the same in the two systems. The difference between  $a_{T,\alpha}$  and  $a_{T,R}$  is the major factor that determines the width of the softening dispersion.<sup>19</sup> Therefore, the widths of the softening dispersions of the two systems are nearly the same, as found experimentally in this study.

## V. Discussion and Conclusions

An explanation of the properties of the softening dispersion of amorphous polymers and their variation in polymers with different chemical structures remains an important fundamental issue in polymer viscoelasticity. The explanation we offered<sup>18–20,22</sup> hinges on the characteristics of the local segmental motions (LSM), which are obviously important factors because they determine the glass temperature  $T_g$  and they depend on the chemical structure of the polymer. The stretched exponential time dependence of the LSM is found to apply not only to mechanical relaxation as for example by eq 2, but also to light scattering,<sup>18,21,22,31</sup> dielectric relaxation,<sup>40</sup> and nuclear magnetic resonance measurements.<sup>41,42</sup> The stretch exponent  $(1 - n_\alpha)$  varies with the chemical structure of the polymer.<sup>37,38</sup> In the coupling model,  $n_\alpha$  is the coupling parameter of the LSM, and its value is proportional to the intermolecular coupling and the intermolecular constraints between the repeat units. Thus,  $n_\alpha$  depends on the chemical structure. A prediction of the coupling model given by eq 3 is that  $n_\alpha$  has a role in determining the temperature dependence of the shift factor of the LSM,  $a_{T,\alpha}$ . There

is a difference between the temperature dependences of  $a_{T,\alpha}$  and  $a_{T,R}$ , the shift factor of the Rouse modes (see eq 4), and this difference is a major factor that determines the width of the softening dispersion. In polymer such as PS that has larger  $n_\alpha$ , the difference is magnified, and consequently the width of the softening dispersion is narrow compared with PIB that has smaller  $n_\alpha$ . The narrower softening dispersion of PS makes it difficult to resolve the sub-Rouse modes, which occurs in between the LSM and the Rouse modes and has intermediate length scales. On the other hand, the much wider softening dispersion of PIB has enabled the sub-Rouse modes to be resolved.

Intermolecular coupling between the repeat units of PS in executing the LSM can be reduced by the addition of a solvent having a lower glass temperature. This modification of PS brings down the value of  $n_\alpha$  and should make the properties of the softening dispersion of the solution approaches that of PIB. At some optimal PS concentration,  $n_\alpha$  of the solution will match  $n_\alpha$  of bulk PIB, and the properties of the softening dispersion of the solution should resemble in many respects to bulk PIB. The data we obtained before at the higher 25% PS concentration and a new measurement on the optimal concentration of 17% PS in TCP verify that these expectations have been realized.

**Acknowledgment.** The work done at the Naval Research Laboratory was supported by the Office of Naval Research. The measurement of the 17% PS solution in TCP were carried out with the support of the National Science Foundation under Grant DMR 95 30372. Dr. In-Chul Chay assisted in the measurements.

## References and Notes

- (1) Tobolsky, A. V. *Properties and Structure of Polymers*; John Wiley and Sons: New York, 1960.
- (2) Ferry, J. D. *Viscoelastic Properties of Polymers*, 3rd ed.; John Wiley & Sons: New York, 1980.
- (3) Aklonis, J. J.; MacKnight, W. J. *Introduction to Polymer Viscoelasticity*, 2nd ed.; John Wiley and Sons: New York, 1983.
- (4) Aklonis, J. J.; Rele, V. B. *J. Polym. Sci., Polym. Symp.* **1974**, *46*, 127.
- (5) Fitzgerald, E. R.; Grandine, L. D.; Ferry, J. D. *J. Appl. Phys.* **1953**, *24*, 650.
- (6) Ferry, J. D.; Grandine, L. D.; Fitzgerald, E. R. *J. Appl. Phys.* **1953**, *24*, 911.
- (7) Catsiff, E.; Tobolsky, A. V. *J. Colloid Sci.* **1955**, *10*, 375.
- (8) Ferry, J. D. *Macromolecules* **1991**, *24*, 5237.
- (9) Plazek, D. J.; Chay, I.-C.; Ngai, K. L.; Roland, C. M. *Macromolecules* **1995**, *28*, 6432.
- (10) Ngai, K. L.; Plazek, D. J. *Rubber Chem. Technol.* **1995**, *68*, 376.
- (11) Okamoto, H.; Inoue, T.; Osaki, K. *J. Polym. Sci., Polym. Phys. Ed.* **1995**, *33*, 1409.
- (12) Ngai, K. L.; Plazek, D. J.; Bero, C. *Macromolecules* **1993**, *26*, 1065.
- (13) Riande, E.; Markovitz, H.; Plazek, D. J.; Raghupathi, N. *J. Polym. Sci., Symp.* **1975**, *50*, 405.
- (14) Cavaille, J.-Y.; Jordan, C.; Perez, J.; Monnerie, L.; Johari, G. *J. Polym. Sci., Part B: Polym. Phys.* **1987**, *25*, 1235.
- (15) Palade, L. I.; Verney, V.; Attené, P. *Macromolecules* **1995**, *28*, 7051.
- (16) Santangelo, P.; Ngai, K. L.; Roland, C. M. *Macromolecules* **1993**, *26*, 2682.
- (17) Williams, M. L. *J. Polym. Sci.* **1962**, *62*, 57.
- (18) Plazek, D. J.; Bero, C.; Neumeister, S.; Floudas, G.; Fytas, G.; Ngai, K. L. *J. Colloid Polym. Sci.* **1994**, *272*, 1430.
- (19) Ngai, K. L.; Plazek, D. J.; Rendell, R. W. *Rheol. Acta* **1997**, *36*, 307.
- (20) Ngai, K. L.; Plazek, D. J.; Echeverria, I. *Macromolecules* **1997**, *29*, 7937.
- (21) Rizos, A. K.; Jian, T.; Ngai, K. L. *Macromolecules* **1995**, *28*, 517.
- (22) Ngai, K. L.; Plazek, D. J.; Rizos, A. K. *J. Polym. Sci., Part B: Polym. Phys.* **1997**, *35*, 599.
- (23) Plazek, D. J.; O'Rourke, V. M. *J. Polym. Sci., Part A-2* **1971**, *9*, 209.
- (24) Ngai, K. L.; Schönhals, A.; Schlosser, E. *Macromolecules* **1992**, *25*, 4519.
- (25) Plazek, D. J.; Schlosser, E.; Schönhals, A.; Ngai, K. L. *J. Chem. Phys.* **1993**, *98*, 6488.
- (26) Plazek, D. J.; Riande, E.; Markovitz, H.; Raghupathi, N. *J. Polym. Sci., Polym. Phys. Ed.* **1979**, *17*, 2189.
- (27) Reissig, S.; Beiner, M.; Korus, J.; Schröter, K.; Donth, E. *Macromolecules* **1995**, *28*, 5394.
- (28) Reissig, S.; Beiner, M.; Vieweg, S.; Schroter, K.; Donth, E. *Macromolecules* **1996**, *29*, 3996.
- (29) Tsang, K. Y.; Ngai, K. L. *Phys. Rev. E* **1996**, *54*, R3067; **1997**, *56*, R17.
- (30) Ngai, K. L.; Tsang, K. Y. *Phys. Rev. E* **1999**, *60*, 4511.
- (31) Patterson, G. D. In *Dynamic Light Scattering*; Pecora, R., Ed.; Academic: New York, 1986; Chapter 6, p 260.
- (32) Miller, J. B.; McGrath, K. J.; Roland, C. M.; Trask, C. A.; Garroway, A. N. *Macromolecules* **1990**, *23*, 4543.
- (33) Roland, C. M.; Ngai, K. L. *Macromolecules* **1991**, *24*, 2261.
- (34) Plazek, D. J.; Raghupathi, N.; Orbon, S. J. *J. Rheol.* **1979**, *23*, 477.
- (35) Ferry, J. D. *Viscoelastic Properties of Polymers*, 3rd ed.; John Wiley & Sons: New York, 1980; Chapter 4, p 91.
- (36) Plazek, D. J.; Zheng, X. D.; Ngai, K. L. *Macromolecules* **1991**, *24*, 1222.
- (37) Plazek, D. J.; Ngai, K. L. *Macromolecules* **1991**, *24*, 1222.
- (38) Böhmer, R.; Ngai, K. L.; Angell, C. A.; Plazek, D. J. *J. Chem. Phys.* **1993**, *99*, 4201.
- (39) Bero, C. Ph.D. Thesis, Department of Materials Science and Engineering, University of Pittsburgh, Pittsburgh, PA, 1997.
- (40) Williams, G.; Watts, D. C. *Trans. Faraday Soc.* **1971**, *66*, 80.
- (41) Spiess, H. W. *J. Non-Cryst. Solids* **1991**, *131–133*, 766.
- (42) Kaufmann, S.; Wefing, S.; Schaefer, D.; Spiess, H. W. *J. Chem. Phys.* **1990**, *93*, 197.

MA0209904